Innovative Petrophysical Model To Interpret Multicomponent Induction Log Data

André Santos, Berthold F. Kriegshäuser, Baker Atlas, Brazil, Rick Mollison, and Liming Yu, Baker Atlas, U.S.A.

Abstract

In this paper we discuss an innovative tensor resistivity petrophysical model to better evaluate the hydrocarbon content of laminated sand-shale sequences. This new approach utilizes horizontal and vertical resistivities computed from multicomponent induction log data in combination with the Thomas-Stieber volumetric model to properly estimate the hydrocarbon content of these laminated reservoirs. Laminated sand-shale reservoirs are routinely encountered in deepwater turbidite environments. Detection and accurate characterization of these reservoirs are challenging using conventional resistivity data and traditional interpretation methodology. Conventional horizontal resistivity data is dominated by the highly conductive shale component of a laminated sequence due to the 'resistors-in-parallel' effect. The vertical resistivity, however, measured perpendicular to the bedding exhibits a strong sensitivity to the resistive hydrocarbon-bearing sand laminae due to the 'series-resistior' effect. Incorporating both horizontal and vertical resistivity data together with the volumetrically consistent Thomas-Stieber model provides a more reliable and robust hydrocarbon estimate when compared to conventional methodologies.

Introduction to Low-Resistivity Pay Problem

Thinly laminated sand-shale sequences are routinely encountered in hydrocarbon exploration and production. The deepwater reservoirs from the Campos Basin, for example, can be very complex and heterogeneous, ranging from massive sands to highly laminated sand-shale sequences (Gomes, et al., 2002). If the thickness of the sand-shale laminae is less than the vertical resolution of the wireline instrument (i.e., gamma ray, density, etc.), the 'scalar' tool response becomes a volume weighted bulk measurement and the intrinsic properties of the individual components can no longer be determined using conventional methodology. In wells drilled approximately perpendicular to bedding, conventional induction tools measure only the horizontal resistivity which is dominated by the highly conductive shales. This gives rise to the classic 'low contrast, low resistivity' shaly sand evaluation problem where economic 'pay' may be only a few tenths of an Ohm-m greater than the shale resistivity. Accurately determining shale volume and water saturation with traditional methodologies is problematic, particularly in costly exploration and development scenarios.

Thinly bedded sand-shale sequences exhibit significant macroscopic electrical anisotropy when the sands are hydrocarbon bearing because the resistivity parallel to bedding is less than the resistivity perpendicular to bedding and resistivity becomes a 'tensor' property with a directional dependency. By incorporating this physical property through the use of vertical and horizontal formation resistivities in the petrophysical model, we can more accurately determine the laminar sand fraction resistivity and laminar shale volume (Mollison, et al., 1999, Schön, et al., 1999). The addition of vertical resistivity greatly enhances the qualitative detection of hydrocarbon-bearing zones using the electrical anisotropy response.

The new multicomponent induction logging tool (3DEX^{SM}) (Beard, et al., 1998, Kriegshäuser, et al., 2000) provides all necessary measurements to derive both horizontal and vertical resistivities regardless of formation dip or wellbore deviation. The horizontal and vertical conductivities can be computed from multicomponent induction log data (Yu, et al., 2001).

In this paper we will

- Review the tensor resistivity petrophysical model.
- Demonstrate resistivity model with uncertainty analysis.
- Discuss interpretation problems of electrical anisotropy.

Tensor Resistivity Model

In a layered formation composed of conductive shale and hydrocarbon bearing sands, if the thickness of the individual laminae is less than the vertical resolution of the induction instrument, these sequences will exhibit macroscopic electrical anisotropy and the physical property of conductivity (σ or $1/R$) is directionally dependent. The horizontal and vertical tool responses, σ_h and σ_v, in a layered sand-shale sequence can be calculated as a function of laminar shale volume (Klein, et al., 1997) from the parallel and series conductivity equations as

$$\sigma_h = \sigma_{sh} V_{shl} + \sigma_{sd} V_{sd}\,, \tag{1}$$

$$\frac{1}{\sigma_v} = \frac{V_{shl}}{\sigma_{sh}} + \frac{V_{sd}}{\sigma_{sd}}\,, \tag{2}$$

and

$$1 = V_{sd} + V_{shl}\,. \tag{3}$$

σ_{sh} and σ_{sd} are the shale and sand conductivities and V_{shl} and V_{sd} are the corresponding laminar shale and sand volume fractions. We also define the anisotropy ratio as

$$\lambda_{ratio} = \frac{\sigma_h}{\sigma_v} = \frac{R_v}{R_h}\,. \tag{4}$$

In this context, horizontal and vertical conductivity, σ_h and σ_v, and their inverse, R_h and R_v, are always defined as parallel and perpendicular to bedding, respectively (see Figure 1).

From the conductivity and volumetric response Equations (1), (2) and (3) above, four cases are possible depending on the intrinsic properties of the sand and shale components:

A. Sand and shale are both isotropic.
B. Anisotropic shale and isotropic sand.
C. Anisotropic sand and isotropic shale.
D. Sand and shale are both anisotropic.

We will focus on the most common case B, anisotropic shale and isotropic sand and show that case A is a subset of case B where the horizontal and vertical shale conductivities are equal, i.e., $\sigma_{shh} = \sigma_{shv}$. Cases C and D, which deal with anisotropic sand, are beyond the scope of this paper and we refer the reader to Schön, et al., 1999, 2000, for a detailed discussion.

In the most common case, the sand conductivity, σ_{sd}, and the laminated shale content, V_{shl}, can be calculated from Equations (1), (2) and (3) (Mollison, et al., 1999) using the macroscopic formation conductivities, σ_h and σ_v, and assuming that we can estimate shale conductivities, σ_{shh} and σ_{shv}, from adjacent massive shales, as

$$\sigma_{sd} = \frac{1}{2}\left[(\sigma_{sd_{app}} + \sigma_{shh}) \pm \sqrt{(\sigma_{shh} - \sigma_{sd_{app}})^2 (1 + \Delta\sigma)}\right], \quad (5)$$

where

$$\sigma_{sd_{app}} = \sigma_v \frac{\sigma_{shh} - \sigma_h}{\sigma_{shv} - \sigma_v}, \quad (6)$$

$$\Delta\sigma = 4\sigma_{sd_{app}} \frac{\sigma_{shh} - \sigma_{shv}}{(\sigma_{sd_{app}} - \sigma_{shh})^2}, \quad (7)$$

and

$$V_{shl} = \frac{\sigma_h - \sigma_{sd}}{\sigma_{shh} - \sigma_{sd}}, \quad (9)$$

or

$$V_{shl} = \frac{\sigma_{shv}}{\sigma_v} \frac{\sigma_v - \sigma_{sd}}{\sigma_{shv} - \sigma_{sd}}. \quad (10)$$

Equation (6) is defined as the "apparent sand conductivity", since this equation results directly from Equations (1), (2) and (3) for the solution of σ_{sd} if the shale is isotropic, (i.e., $\sigma_{shh} = \sigma_{shv}$),

$$\sigma_{sd} = \sigma_v \frac{\sigma_{sh} - \sigma_h}{\sigma_{sh} - \sigma_v}. \quad (11)$$

Petrophysical Model

The petrophysical model incorporates horizontal and vertical resistivity data combined with the Thomas-Stieber (1975) sand-shale volumetric model to better evaluate low contrast, low-resistivity pay zones such as laminated, thin-bedded sequences. Details of the petrophysical model are discussed in Mollison, et al., 1999, 2000, Schön, et al., 1999, and Page, et al., 2001. The model is summarized in the following steps:

1. A total shale volume is determined from classical shale estimators (e.g., gamma ray, SP, density-neutron crossplot, etc.)
2. Total porosity is computed from either bulk density or a combination of density and neutron in the presence of light hydrocarbons. Total porosity and clay bound water volume from NMR data may be directly input as well.
3. Laminar shale volume is computed independently from the tensor resistivity data, σ_v and σ_h, and the Thomas Stieber volumetric shale distribution model.
4. Laminar shale volumetric effects are removed from the bulk volumetrics resulting in a normalized 'sand referenced' total and effective porosity.
5. Dispersed shale volume is computed as the difference of total and laminar shale volumes and is normalized to the 'sand referenced' volume. This allows the computation of the sand fraction effective porosity and clay bound water.
6. Total water saturation of the sand fraction is computed using the Waxman-Smits (1968) equation and Qv_{sd} is computed from the sand-normalized dispersed shale bound water saturation (Thomas-Haley, 1977) using the Hill, Shirley, Klein (1979) equation. If the sands are clean, Archie's equation can be used.
7. Results of the 'sand referenced' volumetrics are re-normalized to formation bulk volumes by a factor of ($1-V_{shl}$), the sand fraction bulk volume, thus allowing computation of bulk hydrocarbon volumes, porosity-feet, N/G, etc.

Determination of Sand Porosity and Water Saturation

To avoid interpretation errors, it is important to clearly differentiate between bulk volumes, referred to as a fraction of the total rock, and the laminar 'sand referenced' volumes, referred to as the laminar sand fraction of the binary formation normalized to 100% sand volume. Throughout the text, we will use the subscript '*sd*' to refer to the 'sand referenced' or laminar sand normalized volumes. Also note that by directly solving for the sand conductivity in Equation (5) and using the Thomas-Stieber 'sand referenced' porosities, we have removed all non-reservoir laminar shale effects, thus reducing the shaly sand analysis to a single 'dispersed' clay/shale problem. If authigenic clays are present, then CEC data is required for the most accurate solution. However, if this data is not available, then the assumption of 'dispersed shale' made in the Thomas-Stieber model can provide a 'first approximation' of dispersed clay conductivity effects. If the sands are clean, then Archie's equation can be used. The water saturation using sand referenced volumetrics is:

$$S_{wt_{sd}}^{n^*} = \left[\frac{a^* \times s_{sd}}{f_{t_{sd}}^{m^*} \times (s_w + B \times Q_{v_{sd}} \times S_{wt_{sd}}^{-1})}\right], \quad (12)$$

where

$$f_{t_{sd}} = \frac{f_t - f_{sh} \times V_{shl}}{(1 - V_{shl})}. \quad (13)$$

Qv_{sd} can be determined from the Hill, Shirley, Klein (1979) equation as shown here where $NaCl$ is the salinity of the formation water.

$$Q_{v_{sd}} = \frac{S_{wbd_{sd}}}{\left(\frac{0.6425}{\sqrt{NaCl_{kppm}}} + 0.22\right)}, \quad (14)$$

where

$$S_{wb_{sd}} = \frac{f_{CBWD_{sd}}}{f_{t_{sd}}}. \quad (15)$$

Error And Uncertainty Propagation

The new petrophysical model results in a more robust evaluation of the hydrocarbon volume in low-resistivity pay sands by using both R_h and R_v (i.e., $1/s_h$ and $1/s_v$) to directly solve for both R_{sd} ($1/s_{sd}$) and V_{shl}. Conventional methodology using only R_h and the parallel conductivity relationship, Equation (1), are very susceptable to large errors as the result of small uncertainties in either or both V_{shl} and R_{sh}. Table 1 shows the error propagation for a typical sand-shale scenario for both the conventional and tensor resistivity models. The addition of vertical resistivity in the tensor analysis dramatically reduces the error propagation in R_{sd} and resulting S_w.

Figure 3 illustrates the point that electrical anisotropy is dependent on bed geometry while the Thomas-Stieber relationship is volumetric. If internal bedding is deformed or irregular, the macroscopic electrical anisotropy will be reduced. The second sensitivity analysis demonstrates the reduction in anisotropy if deformation is greater than 15 degrees (see Figures 4 and 5).

Limitations

This petrophysical model is a major improvement in formation evaluation in laminated reservoirs. However, there are limitations that must be addressed to further improve our formation evaluation.

- The tensor petrophysical model is two-dimensional and only transverse anisotropy is considered, i.e., the resistivity in the azimuthal direction is not varying. Laminae or beds are assumed to be horizontally or 'laterally' isotropic.
- The analysis is based on the assumption that the shale parameters of the laminated zones are the same as of the bounding shales.
- Auxiliary data are needed if the laminated sand-shale sequences are comprised of anisotropic sands.
- Highly resistive tight calcite streaks can cause anisotropy not associated with hydrocarbon-bearing sands (see Figure 2). These effects must be corrected, i.e., the measured vertical resistivity must be corrected before the petrophysical analysis computes the sand resistivity. Borehole image data or core data can be used as auxiliary data input.

Conclusions

We have developed an innovative petrophysical interpretation model specifically designed for low contrast, low resistivity shaly sand pay zones. The analysis incorporates new resistivity data from 3DEX, a multicomponent induction logging device. By utilizing the horizontal and vertical resistivities measured by 3DEX, the petrophysical analysis computes a more accurate laminar sand resistivity. This sand resistivity is then incorporated in a volumetrically balanced petrophysical model utilizing the Thomas-Stieber shale distribution approach. This model results in a better quantification of hydrocarbons-in-place in low-resistivity pay zones and is more robust when compared with the measurement uncertainties using only horizontal resistivity.

Nomenclature

a^*, m^*, n^*	Waxman-Smits electrical properties
B	Waxman-Smits ion mobility constant
f_t	total porosity
f_{CBWD}	dispersed clay bound water volume
Q_v	CEC per unit total pore volume (meq/cm^3)
R	resistivity, Ohm.m
S_{wt}	total water saturation
S_{wbd}	dispersed shale bound water saturation
V_{shl}	laminar shale volume
s	conductivity, S/m
s_w	formation water conductivity
h	*subscript*, horizontal tensor property
v	*subscript*, vertical tensor property
sd	*subscript*, 'sand referenced' volume

References

Beard, D. R., van der Horst, M., Strack, K. M., and Tabarovsky, L. A., 1998, "Electrical logging of a laminated formation," International Patent WO 98/00733.

Gomes, R.M., Denicol, P.S., da Cunha, A.M.V., de Souza, M.S., Kriegshäuser, B., Payne, C.J., and Santos, A., 2002, "Using multicomponent induction log data to enhance formation evaluation in deepwater reservoirs from Campos Basin, Offshore Brasil," paper N, SPWLA 43rd Annual Logging Symposium Transactions.

Hill, H.J., Shirley, O.J., and Klein, G.E., 1979, "Bound Water In Shaly Sands - Its Relation to Qv And Other Formation Properties," Edited by M.H. Waxman and E.C. Thomas, The Log Analyst, Vol. XX, No.3, May-June.

Juhasz, I., 1981, "Normalized Qv - The Key to Shaly Sand Evaluation Using The Waxman-Smits Equation in the Absence of Core Data," paper Z, SPWLA 22nd Annual Logging Symposium Transactions.

Juhasz, I., 1986, "Porosity Systems And Petrophysical Models Used In Formation Evaluation," SPWLA London Chapter – Porosity Seminar, Oct. 9th, 1986.

Klein, J.D., Martin, P.R. and Allan D.F., "The Petrophysics of Electrically Anisotropic Reservoirs," The Log Analyst, May-June, 1997, pp. 25-36.

Kriegshäuser, B., Fanini, O., Forgang, S., Itskovich, G., Rabinovich, M, Tabarovsky, L., Yu, L., Epov, M., and v. d. Horst, J., 2000, "A new multicomponent induction logging tool to resolve anisotropic formations," paper D, SPWLA 40th Annual Logging Symposium Transactions.

Mollison, R., Schön, J., Fanini, O., Kriegshäuser, B., Meyer, H., and Gupta, P., 1999, "A model for hydrocarbon saturation estimation from an orthogonal tensor relationship in thinly laminated anisotropic reservoirs," paper OO, SPWLA 40th Annual Logging Symposium Transactions .

Mollison, R.A., Ragland, T.V., Schön, J.H., Fanini, O.N., and van Popta, J., 2000, "Reconciliation Of Waxman-Smits And Juhasz 'Normalised Q_v' Models From A Tensor Petrophysical Model Approach Using Field Data," paper YY, SPWLA 41st Annual Logging Symposium Transactions.

Page, G., Fanini, O., Kriegshäuser, B., Mollison, R., Yu, L., and Colley, N., 2001, "Field example demonstrating a significant increase in calculated Gas-In-Place: An enhanced shaly sand reservoir characterization model using 3DEX multicomponent induction data," SPE 71724, Trans. SPE ATCE.

Schön, J. H., Mollison, R. A., and Georgi, D. T., 1999, "Macroscopic electrical anisotropy of laminated reservoirs: A tensor resistivity tensor model," SPE 56509, Trans. SPE ATCE.

Thomas, E.C., and Haley, R.A., 1977, "Log Derived Shale Distribution In Sandstone And Its Effect Upon Porosity, Water Saturation And Permeability," paper N, CWLS 6th Annual Formation Evaluation Symposium Transactions.

Thomas, E.C., and Stieber, S.J., 1975, "The distribution of shale in sandstones and its effect upon porosity," paper T, SPWLA 16th Annual Logging Symposium Transactions.

Waxman, M.H. and Smits, L.J., 1968, "Electrical conductivities in oil-bearing shaly sands," SPE-1863-A, Trans. SPE ATCE.

Yu, L., Kriegshäuser, B., Fanini, O., and Xiao, J., 2001, "A fast inversion method for multicomponent induction log data," 71st Ann. Internat. Mtg., Soc. Expl. Geophys., Expanded Abstracts.

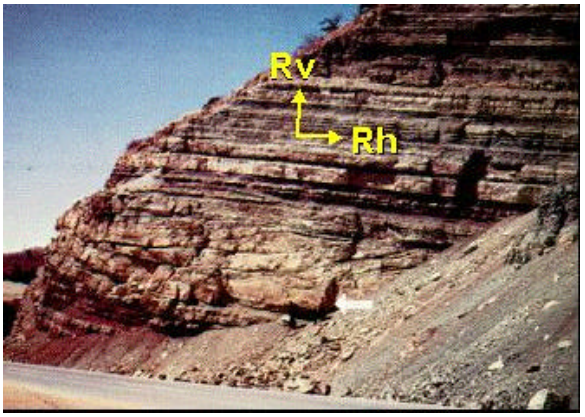

Figure 1. Outcrop photo illustrating the relationship of horizontal and vertical resistivity to formation bedding. Horizontal resistivity is always referenced parallel to bedding and vertical resistivity is always referenced perpendicular to bedding.

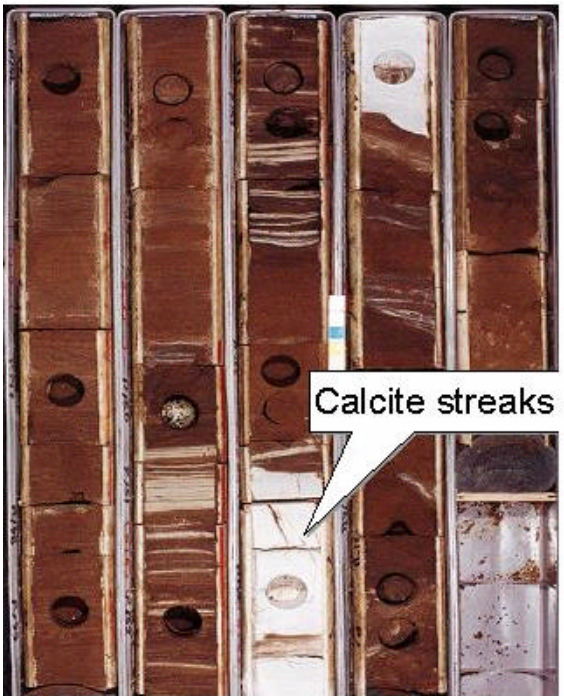

Figure 2. Photos of slabbed whole core with oil saturated sands (brown) and tight, high resistivity limestone laminae and thin beds (white). The thin calcite laminae in the upper center of the photo add significant electrical anisotropy that is unrelated to the sand properties (i.e., hydrocarbon saturation). Additional information such as whole core or resistivity image data is required to properly correct the vertical resistivity in this instance.

True Rsd	Rsh	Rh	Rv	V_{shlamr}	Conventional			3DEX		
					Derived Rsd	Relative Error %		Derived Rsd	Relative Error %	
						Rsd	Sw_{sd}		Rsd	Sw_{sd}
10	1	1.818	5.5	0.5+0.05	8181	-81710	96.5	10	0	0
10	1	1.818	5.5	0.5-0.05	5.5	45	34.8	10	0	0
10	1+0.1	1.818	5.5	0.5	5.2	48	38.7	11.1	-11	5.1
10	1-0.1	1.818	5.5	0.5	-90.9	100.9	66.8	9.1	9	4.8
10	1	1.8+0.18	5.5	0.5	99	-890	68.2	9.1	9	4.8
10	1	1.8-0.18	5.5	0.5	4.3	57	52.5	11.8	-18	7.9
10	1	1.818	5.5+0.55	0.5	10	0	0	11.2	-12	5.5
10	1	1.818	5.5-0.55	0.5	10	0	0	8.8	12	6.6

Rsd Relative Error %

$$\frac{R_{sd\ true} - R_{sd\ derived}}{R_{sd\ true}} \times 100$$

Sw Relative Error %

$$\frac{S_{w\ true} - S_{w\ derived}}{S_{w\ true}} \times 100 = \frac{\sqrt{R_{sd\ derived}} - \sqrt{R_{sd\ true}}}{\sqrt{R_{sd\ derived}}} \times 100$$

Table 1. Error analysis of a hypothetical laminated formation composed of 1 Ohm-m shale and 10 Ohm-m sand. Resulting R_{sd} (i.e., $1/s_{sd}$) and V_{shl} using the conventional parallel conductivity equation solution for R_{sd}, Equation (1), compared to the tensor resistivity model, Equation (11). Both sand and shale are assumed to be isotropic in this model.

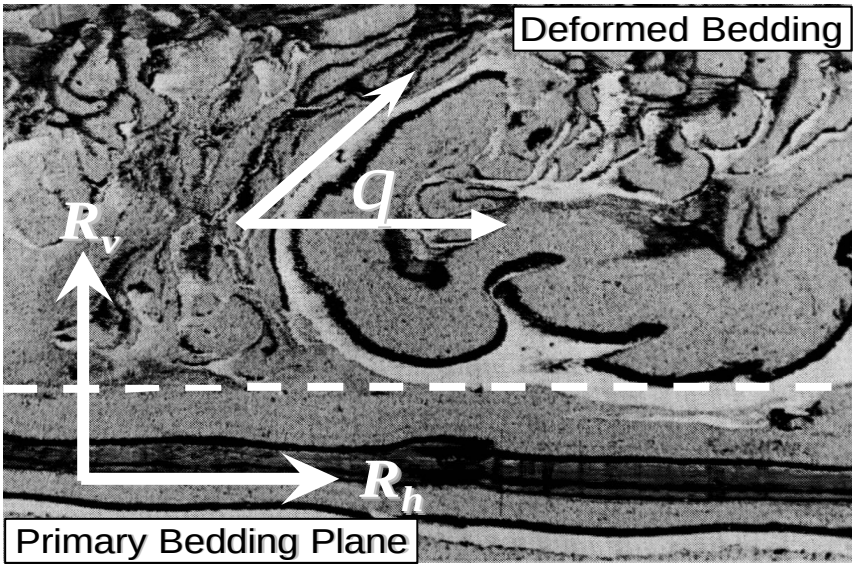

Figure 3. This figure illustrates the problem of bed deformation (upper 2/3rd). Electrical anisotropy is dependent on bed geometry (lower 1/3rd) and deformation of bedding will reduce anisotropy. The Thomas-Stieber volumetric model is not dependent on geometry and this is still a 'laminated formation' because bedding has only been distorted. The sands and shales have not been mixed to form a homogenous 'dispersed shaly sand', thus changing the 'volumetric' shale distribution.

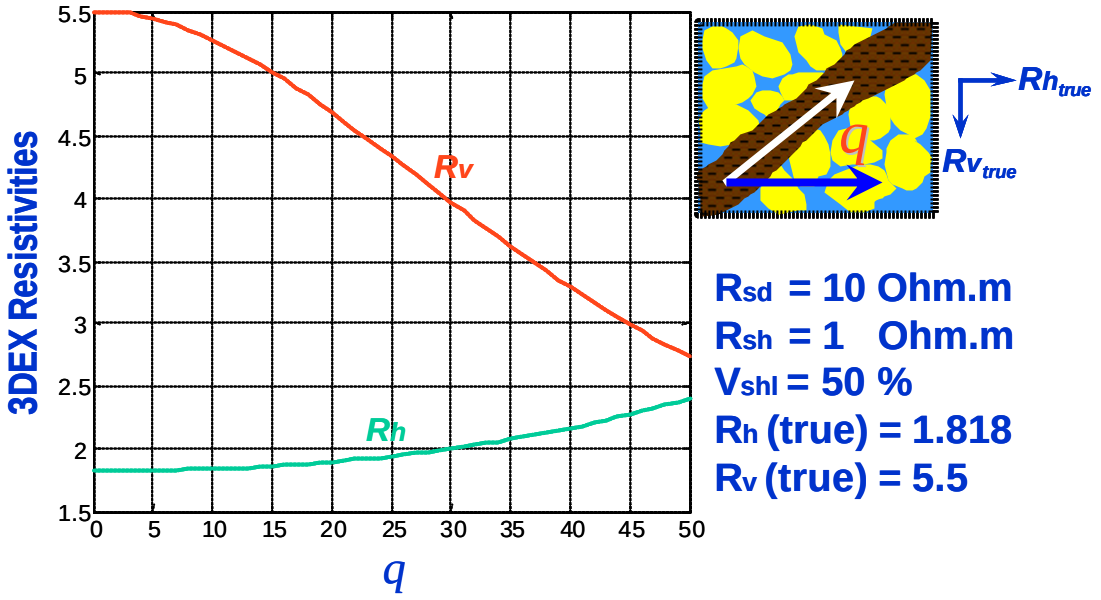

Figure 4. This figure illustrates the resulting error in the horizontal and vertical resistivity, R_h and R_v, (i.e., $1/s_h$ and $1/s_v$), caused by an increasing bed angle due to the internal bed deformation. The model uses the same hypothetical 1 Ohm-m shale and 10 Ohm-m sand laminated formation with equal volumes of sand and shale (maximum anisotropy).

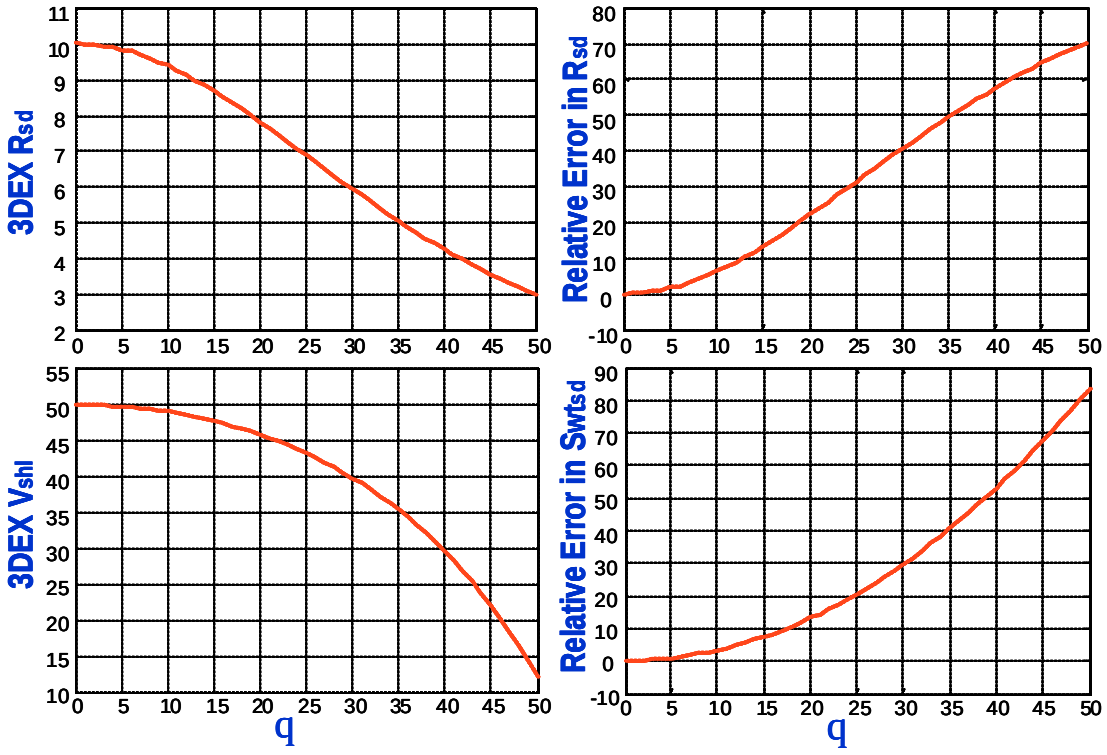

Figure 5 . These figures depict the petrophysical model errors resulting from the R_h and R_v, (i.e., $1/s_h$ and $1/s_v$), errors shown in Figure 4 as a result of an increasing angle of the bed deformation. These errors are propagated through the petrophysical analysis to the computed tensor resistivity, R_{sd} (i.e., $1/s_{sd}$) and V_{shl} , and the resulting relative error in R_{sd} and $S_{wt_{sd}}$.